i-tRAP (individual tRNA acylation PCR): a convenient method for selective quantification of tRNA charging

YUSUKE TSUKAMOTO,[1,2] YUMI NAKAMURA,[1,2] MAKOTO HIRATA,[3] RYUICHI SAKATE,[3] and TOMONORI KIMURA[1,2,3,4]

[1]Reverse Translational Research Project, Center for Rare Disease Research, National Institutes of Biomedical Innovation, Health and Nutrition (NIBIOHN), Ibaraki, Osaka, 567-0085, Japan

[2]KAGAMI Project, National Institutes of Biomedical Innovation, Health and Nutrition (NIBIOHN), Ibaraki, Osaka, 567-0085, Japan

[3]Labaratory of Rare Disease Resource Library, Center for Rare Disease Research, National Institutes of Biomedical Innovation, Health and Nutrition (NIBIOHN), Ibaraki, Osaka, 567-0085, Japan

[4]Graduate School of Medicine, Osaka University, Suita, Osaka, 565-0871, Japan

ABSTRACT

Each transfer RNA (tRNA) is aminoacylated (charged) with a genetic codon-specific amino acid at its 3′ end. Charged tRNAs are primarily used for translation, whereas fluctuations in charged tRNA fractions are known to reflect cellular response to stress. Here we report the development of individual tRNA-acylation using PCR (i-tRAP), a convenient PCR-based method that can specifically quantify the individual tRNA charging ratio. In this i-tRAP method, demethylases remove base methylations which are problematic for reverse transcription reaction, and β-elimination reaction specifically removes the 3′ end of adenine residue in uncharged tRNA. Subsequent TaqMan MGB qRT-PCR can distinguish between cDNA of charged tRNA and uncharged tRNA. By using this method, we revealed that the charging ratio of $tRNA^{Gln}$(CUG) was changed in response to amino acid starvation and also the charging ratio of $tRNA^{Gln}$(CUG) in senescent cells was lower than in young cells under starvation conditions. i-tRAP can be applicable to the quantification of the charging ratio of various tRNAs, and provides a simple and convenient method for analyzing tRNA charging.

Keywords: PCR; aminoacylation; charging; quantification; tRNA

INTRODUCTION

The central dogma of molecular biology is the sequential flow of information from genes to proteins (Crick 1958). In protein biosynthesis, transfer RNA (tRNA) delivers a specific amino acid to its corresponding codon of messenger RNA (mRNA). This specificity of tRNA is key to the interpretation of the genetic code (Crick 1970), which consists of 61 sense triplet codons that encode 20 amino acids. Remarkably, the eukaryote genome possesses a large number of tRNA genes. More than 500 tRNA genes have been identified in the human genome to date (Chan and Lowe 2016). The identity of each mature tRNA produced from those genes is defined by its binding amino acid and its anticodon sequence. tRNA isoacceptors have different anticodons that carry the same amino acid, whereas tRNA isodecoders share the same anticodon but have different sequences (Goodenbour and Pan 2006). tRNA biochemically acts as an acceptor of amino acids (Hoagland et al. 1958). The ribonucleotide sequence of the 3′ end, CCA, is constant among all tRNAs, and the 3′ terminal adenylate ribonucleotide is "charged" with an amino acid via acylation by aminoacyl-tRNA synthetase (aaRS) as reviewed in (Rubio Gomez and Ibba 2020). The tRNA-charged amino acid is then incorporated into a protein during translation, and the tRNA is discharged for subsequent recharging.

The charging ratio of tRNA, that is, the proportion of tRNAs that are charged with amino acids (Morris and DeMoss 1965; Evans et al. 2017), is closely related to several biological phenomena and diseases (Sørensen 2001; Zhou et al. 2009). The charging ratios of the tRNA vary in response to amino acid starvation (Sørensen 2001; Dittmar et al. 2005), growth conditions (Avcilar-Kucukgoze et al. 2016), and external stress (Zaborske et al. 2009). Alterations in the charging ratios of tRNA are assumed to affect translational efficacy (Elf et al. 2003; Saikia et al. 2016; Pavlova et al.

Corresponding author: t-kimura@nibiohn.go.jp

Article is online at http://www.rnajournal.org/cgi/doi/10.1261/rna.079323.122. Freely available online through the *RNA* Open Access option.

2020). Disease-associated mutations in tRNA and aaRS have been widely characterized (Gong et al. 2014; Kwon et al. 2019), and the charging ratio of tRNA is associated with senescence and cellular activity (Hosbach and Kubli 1979; Webster and Webster 1981; Gabius et al. 1982; Gong et al. 2020). The fraction of charged tRNAs is an important biological parameter.

Several methods have been developed to measure the charging ratios of tRNA (Ho and Kan 1987; Dittmar et al. 2005; Loayza-Puch et al. 2016; Evans et al. 2017; Gobet et al. 2020). Acid-urea polyacrylamide gel electrophoresis followed by northern blot hybridization is commonly used for measuring the charging ratio of tRNA at the isoacceptor level (Ho and Kan 1987). Recently, high-throughput methods to determine tRNA charging ratios were developed based on either microarray (Dittmar et al. 2005) or next-generation sequencing methods (Evans et al. 2017). By utilizing a chemical step that removes the 3′-end adenine residue of uncharged tRNA and an enzymatic step of removing tRNA modification, sequencing of tRNA enables comprehensive determination of the charging ratios of tRNA (Evans et al. 2017). On the other hand, convenient qPCR-based methods are preferable for measuring the charging ratio of an individual tRNA, whereas currently available methods only allow for relative quantification (Loayza-Puch et al. 2016).

In this study, we report the development of individual tRNA-acylation using PCR, termed i-tRAP, a convenient PCR-based method that specifically quantifies the individual tRNA charging ratio. The i-tRAP procedure includes a demethylation step catalyzed by *Escherichia coli* AlkB demethylases, β-elimination step which makes uncharged tRNAs' 3′-end CC while charged tRNAs' 3′-end CCA, and TaqMan-MGB probe quantitative PCR for distinguishing tRNA species and determining charged tRNA fractions. By using this method, we show the dynamics of $tRNA^{Gln}$(CUG) charging which responds to cellular nutrient status. In addition, the charging ratio of $tRNA^{Gln}$(CUG) was markedly lower in senescent cells than in young cells under amino acid starvation conditions. i-tRAP provides a convenient method for quantification of the charging ratio of various tRNA and should be used as a tool for investigations of tRNA charging.

RESULTS

Development of PCR-based detection methods for the charging ratio of tRNA

To investigate dynamic changes in the charging ratios of tRNA, we developed a method termed individual tRNA-acylation using PCR (i-tRAP) (Fig. 1). This method includes the following steps. Extracted tRNA is first subjected to a series of chemical and enzymatic treatments reported previously (Neu and Heppel 1964; Trewick et al. 2002). Extracted small RNA is treated with periodate (IO_4^-) to oxidize the free 3′ end of uncharged tRNAs (Neu and Heppel 1964). After removal of the periodate, β-elimination at basic pH is used to selectively change the oxidized 3′-adenylate ribonucleotide (A) residue to 3′ phosphate at the terminal 3′-cytidylate ribonucleotide (C) residue. This 3′-phosphate is then removed using T4 polynucleotide kinase (PNK), and the 3′-nucleotide of the uncharged tRNA becomes C. The same β-elimination step at basic pH, in turn, deacylates charged tRNAs and makes the 3′-A of the tRNA free of amino acid (Fig. 1A). Next, the resultant tRNA is treated with wild-type and mutant AlkB from *E. coli* as previously reported (Zheng et al. 2015). Reverse transcription of tRNA as a template becomes possible through demethylation of the methyl modifications on the Watson–Crick face of the base (Avcilar-Kucukgoze et al. 2016). The resultant tRNA is ligated to a 5′ adenylated linker using T4 RNA ligase 2 (T4Rnl2). The ligation product is then used as a template for reverse transcription, yielding cDNA. To detect single-nucleotide differences in the sequences of the 3′ end of tRNA, that is, CCA versus CC, we utilized a probe-based qPCR assay. We developed two types of probes that differ in sequence only at the 3′ end of the tRNA: one probe is complementary to the 3′CCA-tRNA labeled with VIC, while the other is complementary to

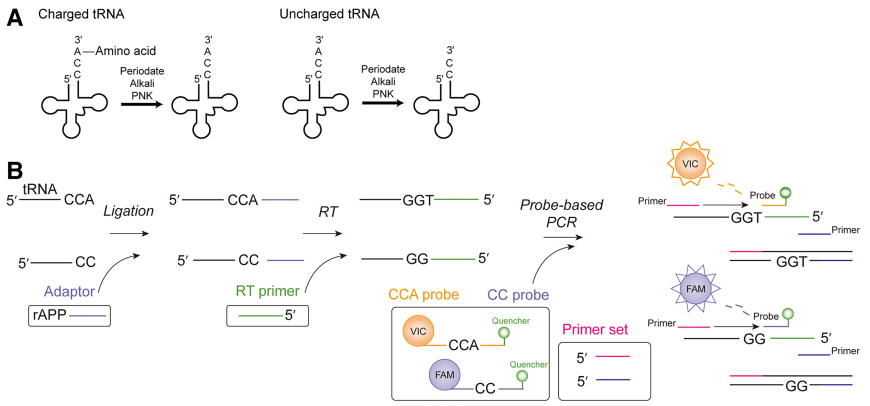

FIGURE 1. Development of i-tRAP, a method for detecting the charging ratio of tRNA. (*A*) Reaction schemes for the pretreatment of tRNA before sequencing. After a series of chemical reactions, charged and uncharged tRNAs are distinguished by 3′-end CCA (3′CCA-tRNA) and CC (3′CC-tRNA), respectively. (PNK) Polynucleotide kinase-3′-phosphatase. (*B*) Scheme of i-tRAP. tRNA pretreated as described above was ligated to an adaptor, reverse-transcribed, and then subjected to a qPCR assay using two probes. During PCR, the *Taq* polymerase degrades the probes and the degradation of the probes results in the releases of either VIC or FAM. The resultant fluorescence signals enable quantification of the amplified products. Fluorescence signals from VIC represent the quantity of 3′CCA-tRNA, whereas those from FAM represent the quantity of 3′CC-tRNA. (RT) reverse transcription.

the 3′CC-tRNA labeled with FAM. Fluorescence signals from VIC and FAM are quenched by quenchers attached to the probes. These probes are also conjugated to minor groove binder (MGB) moieties. MGB moieties increase the melting temperature of their probes by increasing their binding affinity to the target sequences and therefore are generally used for the detection of single-nucleotide polymorphisms (Nagy et al. 2017; Sam et al. 2018). The same concentrations of VIC- and FAM-labeled probes were mixed and used for qPCR. Upon extension using *Taq* polymerase, the probes are degraded and release either VIC or FAM, and the resultant fluorescence signals enable quantification of the amplified products (Fig. 1B). Fluorescence signals from VIC represent the quantity of 3′CCA-tRNA, whereas those from FAM represent the quantity of 3′CC-tRNA.

Validation of i-tRAP by using DNA templates

We selected two tRNA sequences: $tRNA^{Gln}$(CUG) and $tRNA^{Gly}$(GCC). $tRNA^{Gln}$ contains two isoacceptors, $tRNA^{Gln}$(CUG) and $tRNA^{Gln}$(UUG), the former of which has seven isodecoders. We prepared a set of primers and probes for isodecoder #1 of $tRNA^{Gln}$(CUG) (Supplemental Fig. 1A; Supplemental Table S3). The probes contain the isoacceptor-specific sequence of $tRNA^{Gln}$(CUG) and the forward primer contained the isodecoder #1-specific sequence of $tRNA^{Gln}$(CUG), which differed by one to four nucleotides from the sequences of the other. We also prepared a set of primers and probes for isodecoder #1 of $tRNA^{Gly}$(GCC) (Supplemental Fig. 1B; Supplemental Table S3).

For quantitative validation of the i-tRAP method, we prepared tDNAs that contained 3′CCA-tRNA and 3′CC-tRNA sequences by PCR. We first confirmed the specificity of detection of the 3′ end of the tRNA (CC vs. CCA) of this system. For this purpose, tDNA from either 3′CCA-tRNA or 3′CC-tRNA was used as the template for i-tRAP. Real-time plots using a mixture of VIC (to detect 3′CCA-tRNA) and FAM (to detect 3′CC-tRNA) probes revealed that i-tRAP could accurately discriminate between the 3′CCA-tDNA and 3′CC-tDNA sequences (Fig. 2A–D).

Next, we sought to determine whether the fluorescence signal ratios reflect the ratios of 3′CCA-tRNA and 3′CC-tRNA. To this end, we mixed tDNA harboring 3′CCA-tRNA and 3′CC-tRNA sequences at several ratios and used them as templates for i-tRAP. As shown in Figure 2E,F, the ratio of 3′CCA-tRNA-derived tDNA was proportional to the difference in threshold cycle values (ΔC_t) between the FAM and VIC layers ($R^2 = 1.00$ and 0.98, respectively). Of note, the standard curves constructed using different concentrations of templates (0.1–100 attograms) were not different, and therefore, the concentrations of the template in the samples are unlikely to affect quantification (Fig. 2G).

To determine the reaction specificity of i-tRAP against the sequence variations between the isodecoders and isoacceptors, we utilized synthesized tDNAs that contain several sequences of isodecoders and isoacceptors (Fig. 2H). The i-tRAP targeting $tRNA^{Gln}$(CUG) responded to tDNAs of $tRNA^{Gln}$(CTG)-1 (no sequence mismatch for the primer set) and -2 (one mismatch in forward primer with no mismatch in the probe), while fewer responded to tDNAs of $tRNA^{Gln}$(CTG)-6 (no mismatch in forward primer and two mismatches in the probe) and $tRNA^{Gln}$(TTG)-1 (no mismatch in forward primer and one mismatch in the probe). The PCR responses were affected by the sequence mismatches in the MGB probe but not by the mismatches in the forward primer. i-tRAP can distinguish the sequences of isoacceptors of $tRNA^{Gln}$, while it is difficult to distinguish the sequences of isodecorders of $tRNA^{Gln}$.

Validation of i-tRAP by using biological samples

We next verified the quality of the i-tRAP method using biological samples. We first prepared tRNA from HEK293T cells and deacylated the charged tRNA by weak alkali treatment with 200 mM Tris-HCl, pH 8.5, at 37°C for 10 min. i-tRAP indicated that the charging ratios of $tRNA^{Gln}$(CUG) and $tRNA^{Gly}$(GCC) were high under nutrient-rich conditions but were greatly reduced upon weak alkali treatment (Fig. 3A). Northern blot also showed that this treatment reduced the charging ratio of $tRNA^{Gln}$(CUG) and $tRNA^{Gly}$(GCC) (Fig. 3B; Supplemental Fig. 2A,B).

Next, we confirmed the effect of knockdown of *glutaminyl-tRNA synthetase* (*QARS*), which attaches glutamine onto $tRNA^{Gln}$(CUG), on tRNA charging (Fig. 3C). The effects of *QARS* knockdown were confirmed by qRT-PCR (Fig. 3D) and western blotting (Fig. 3E; Supplemental Fig. 2C). Knockdown of *QARS* decreased the charging ratio of $tRNA^{Gln}$(CUG) in cells cultured for 2 d in nutrient-rich medium (Fig. 3F).

We examined if we can further simplify the i-tRAP methods. Recently, a tRNA RT method that does not use demethylase has been reported (Behrens et al. 2021; Watkins et al. 2022). Therefore, we confirmed the necessity of the demethylase treatment and investigated whether these RT methods could be applied to i-tRAP (Supplemental Fig. 2D). When RT was performed using ReverTra Ace, the demethylase treatment intensified the qPCR signals (Supplemental Fig. 2E–H). Regarding the RT enzymes, ReverTra Ace was superior to TGIRT and SuperScript IV in the strength of qPCR signal (Supplemental Fig. 2E–H).

Landscape of tRNA charging reveals the dynamic charging response of $tRNA^{Gln}$ in response to the external amino acid environment

To uncover tRNA charging dynamics, we examined whether charging levels of tRNA respond to nutrient status. For this purpose, we utilized a tRNA sequencing method that

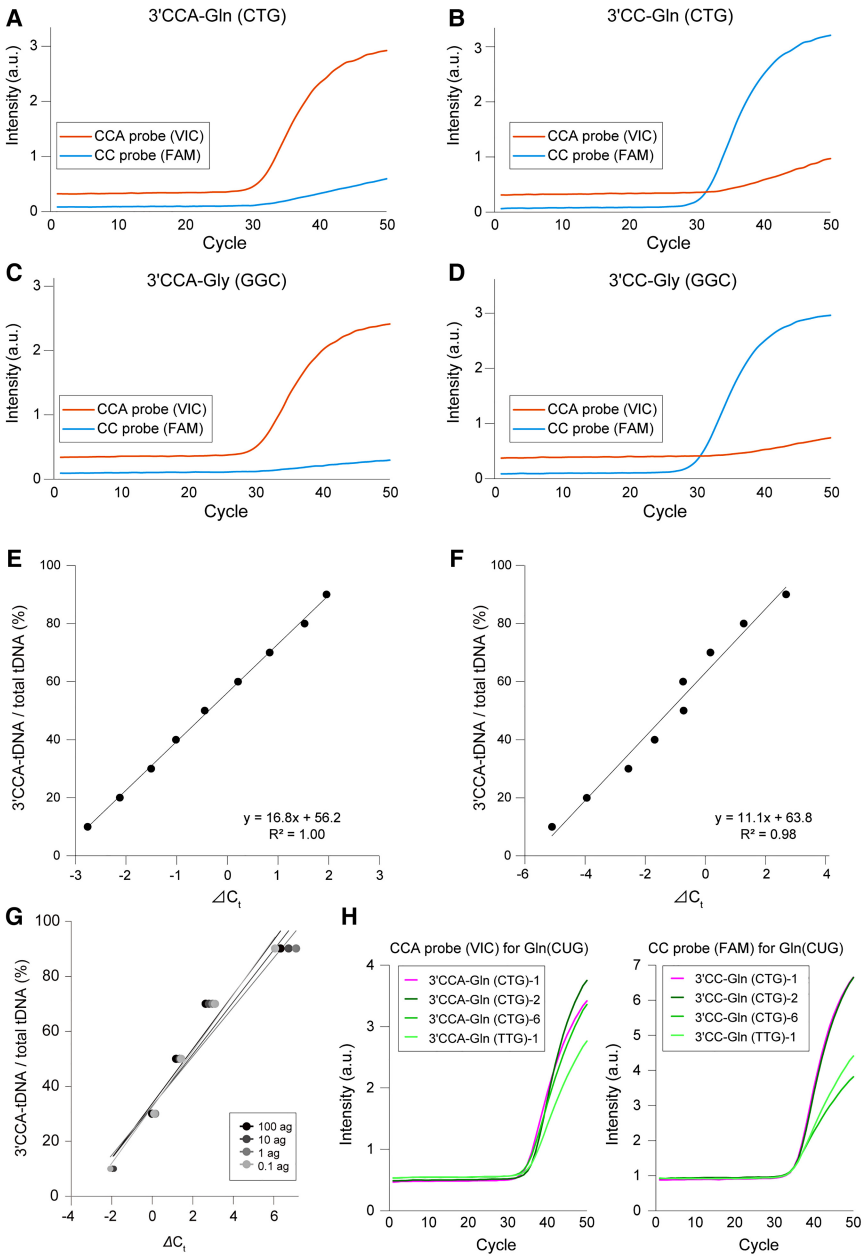

FIGURE 2. Validation of i-tRAP by using synthesized DNA template. (*A–D*) Real-time plots of i-tRAP using 1 ag of the synthesized DNA template, which contains a sequence of either (*A*) 3′CCA-tRNA^{Gln}(CUG), (*B*) 3′CC-tRNA^{Gln}(CUG), (*C*) 3′CCA-tRNA^{Gly}(GCC), or (*D*) 3′CC-tRNA^{Gly}(GCC). Orange lines indicate the VIC signal derived from the CCA probe, and blue lines indicate the FAM signal derived from the CC probe. (*E*,*F*) Standard curve of ΔCt values derived from VIC and FAM signals plotted against the 3′CCA-tDNA ratio of (*E*) tDNA^{Gln}(CTG) and (*F*) tDNA^{Gly}(GGC). Mixed 1 ag of the tDNA templates harboring 3′CCA-tDNA or 3′CC-tDNA at several ratios were used. (*G*) Standard curves of ΔCt values using different concentrations of templates. Standard curves of ΔCt values derived from VIC and FAM signals plotted against the 3′CCA ratio of tDNA^{Gln}(CTG) with different concentrations of templates. Synthesized tDNAs were used as templates. (*H*) Real-time plots of i-tRAP using 1 ag of the synthesized tDNA, which contains a sequence of either tRNA^{Gln}(CUG)-1, 2, 6, or tRNA^{Gln}(UUG)-1. (*Left* panel) VIC signal derived from the CCA probe using 1 ag of 3′CCA-tDNA. (*Right* panel) FAM signal derived from the CC probe using 1 ag of 3′CC-tDNA.

determines charging ratios (Evans et al. 2017) and comprehensively profiled the charging status of tRNAs in response to amino acid supplementation. The effects of amino acid supplementation on tRNA charging profiles were examined using TIG-1 cells (Ohashi et al. 1980). TIG-1 cells are human diploid fibroblasts naturally established without artificial immortalization and are used as a cellular senescence model because they stop dividing at advanced passages. We utilized TIG-1 cells that were young (population doubling level [PDL] 30) or old (PDL 50) and cultured them under amino acid starvation conditions (Fig. 4A). tRNA sequencing revealed that the charging ratio of most tRNAs was 80%–90% upon amino acid supplementation in young and old cells. The low charging ratios of tRNA^{Ser} (Young; 76%, Old; 77%, in mean values) even under amino acid–rich conditions were as previously reported (66%, in a previous report; Evans et al. 2017). tRNA sequencing also revealed that a subset of tRNAs, tRNA^{Gln}, tRNA^{Ser}, and tRNA^{Thr}, exhibited low charging ratios in response to amino acid starvation (Fig. 4B). Among them, tRNA^{Gln} displayed the largest change in response to amino acid starvation (amino acid supplementation vs. amino acid starvation: Gln(UUG); 93% vs. 60%, Gln(CUG); 94% vs. 37%, mean values, Fig. 4B). Although, in the presence of abundant amino acids, tRNA charging ratios were identical between aged and young cells (Fig. 4B), the charging ratio of tRNA^{Gln}(UUG) and tRNA^{Gln}(CUG) were markedly lower in senescent cells in response to amino acid starvation (Fig. 4B). We measured the charging ratio of tRNA^{Gln}(CUG) and tRNA^{Gly}(GCC) by i-tRAP using tRNAs from TIG-1 cells cultured in medium with or without amino acids. i-tRAP revealed that the charging ratio of tRNA^{Gln}(CUG) was significantly decreased by amino acid starvation, whereas the ratio of tRNA^{Gly}(GCC) was unchanged (Fig. 4C), confirming the tRNA sequencing results (Fig. 4B). Together, these findings validate the

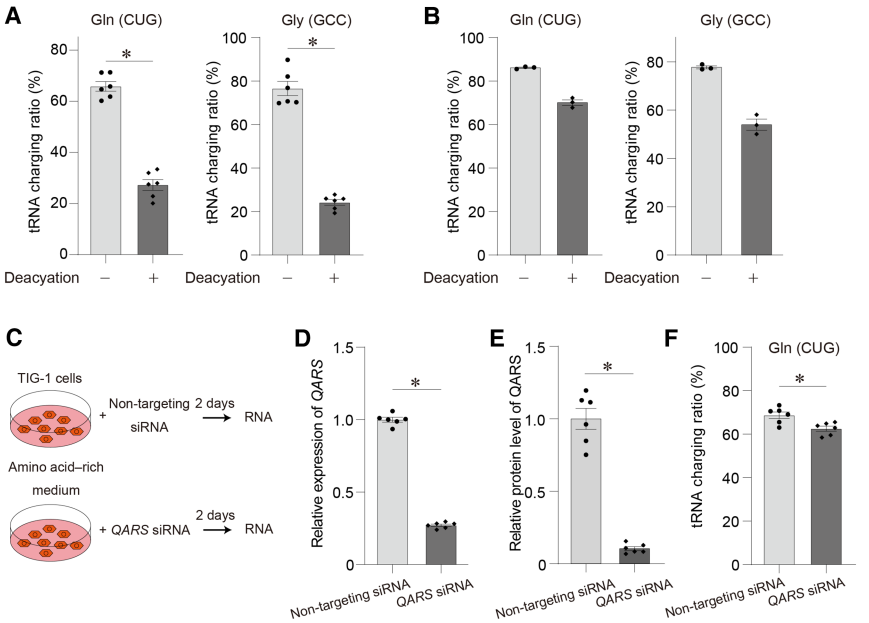

FIGURE 3. Validation of i-tRAP by using biological samples. (*A*) Effects of weak alkali treatment on the charging ratios of tRNA^{Gln}(CUG) (*left*) and tRNA^{Gly}(GCC) (*right*). tRNA charging levels were quantified by using i-tRAP. Small RNA was extracted from HEK293T cells and deacylated the charged tRNA by weak alkali treatment with 200 mM Tris-HCl, pH 8.5, at 37°C for 10 min. (*B*) Northern blot quantification of tRNA^{Gln}(CUG) and tRNA^{Gly}(GCC) aminoacylation. Aminoacylation of tRNA^{Gln}(CUG) and tRNA^{Gly}(GCC) were analyzed by acid-urea gel electrophoresis and subsequent northern blot hybridization using probes for tRNA^{Gln}(CUG) and tRNA^{Gly}(GCC), respectively. tRNA charging levels were quantified as a ratio of charged-to-total tRNA. (*C*) Experimental scheme for panels *D*–*F*. TIG-1 cells cultured in an amino acid–rich medium were transfected with the indicated siRNAs and cultured for an additional 2 d. (*D*) *QARS* gene expression, (*E*) quantification of QARS by western blot, and (*F*) charging ratio of tRNA^{Gln}(CUG). Data, mean ± SEM; $n = 3$ (*B*) and 6 (A, D, E, and F); statistics, (A, D, E, and F) unpaired two-tailed Student's *t*-test. (*) $P < 0.05$.

ability of the i-tRAP method to quantify the charging ratios of tRNA. Additionally, the i-tRAP method developed herein has advantages in terms of ease and convenience. Among the two types of tRNA^{Gln} codons, tRNA^{Gln}(CUG) responded more strongly to amino acids, and these results were replicated using acid-urea polyacrylamide gel electrophoresis followed by northern blotting (Fig. 4D; Supplemental Fig. 3A,B). i-tRAP also revealed that the charging ratio of tRNA^{Gln}(CUG) in old cells was significantly lower than in young cells under amino acid starvation (Fig. 4E). Therefore, a reduced tRNA^{Gln} (CUG) charging ratio in response to starvation is a feature of old/senescent cells.

Charging ratio of tRNA^{Gln}(CUG) dynamically responds to external amino acids

We evaluated the dynamics of the charging of tRNA^{Gln}(CUG). We first investigated when the charging ratio of tRNA^{Gln}(CUG) decreases upon amino acid starvation (Supplemental Fig. 4A). Under amino acid–rich conditions, the charging ratio was 77.5% (SEM = 0.98), which was decreased to 27.3% (SEM = 1.9) after 15 h of starvation (Fig. 5A). The decrease in the charging ratio occurred between 3 and 6 h after starvation. On the other hand, the charging ratio of tRNA^{Gly}(GCC) was maintained after 15 h of starvation (Fig. 5A). Expression levels of *QARS* were unchanged (Supplemental Fig. 4B). The decrease in tRNA charging did not correlate with the expression levels of *QARS*.

Next, we investigated the recharging process of tRNA^{Gln}(CUG) by supplying amino acids. After 15 h of starvation, we supplied amino acids to the medium and measured the tRNA charging ratio (Supplemental Fig. 4C). The decreased charging ratio increased 15 min after supplying amino acids (Fig. 5B), while expression levels of *QARS* increased slightly 180 min after the addition of amino acids (Supplemental Fig. 4D). These results suggest that the restoring process of tRNA charging is faster than the decreasing process of the charging ratio of tRNA.

We next examined substrate specificity for the charging process. Supplementation with glutamine alone or with all amino acids except glutamine for 1 h increased the charging ratio of tRNA^{Gln}(CUG) after starvation (Fig. 5C). This result suggests that amino acids other than glutamine might be converted to compensate for glutamine depletion. To determine the effect of extracellular glutamine on the charging ratio of tRNA^{Gln}(CUG), the cells were treated in a dose-dependent manner with glutamine for 1 h after starvation. Treatment with at least 2 μM extracellular glutamine resulted in an increased charging ratio of tRNA^{Gln}(CUG) (Fig. 5D). Although there was no statistically significant difference, the mean value of the charging ratio of tRNA^{Gln}(CUG) increased in a dose-dependent manner.

DISCUSSION

In this study, we developed the i-tRAP method, a convenient PCR-based method that specifically quantifies the individual tRNA charging ratio. By using this method, we showed that the charging ratio of tRNA^{Gln} (CUG) was lower in old cells than in young cells under starvation conditions and the charging ratio of tRNA^{Gln} (CUG) was responsive to amino acid levels.

The i-tRAP method developed herein has advantages in ease and convenience. To date, several methods have

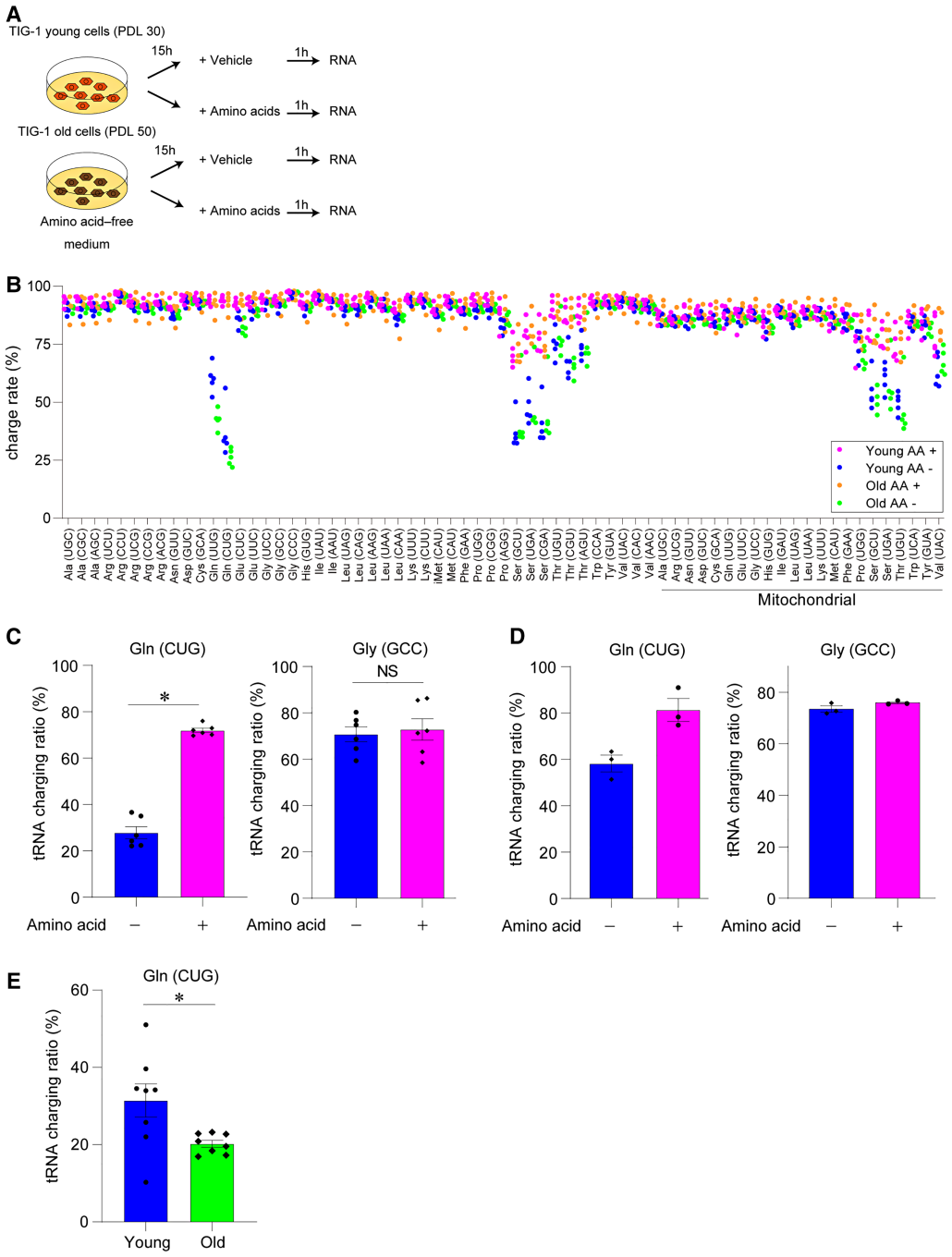

FIGURE 4. Landscape of tRNA charging reflects nutrient status. (*A*) Experimental scheme. Young and old TIG-1 cells were cultured in an amino acid–free medium, which was replaced with a medium containing amino acids or not. After a 1 h incubation, cells were collected and RNA was extracted. (*B*) Charging ratios of tRNAs in amino acid-supplied (Young AA +; magenta, Old AA +; orange) and –starved conditions (Young AA –; cyan, Old AA –; green) plotted based on codon. $n = 5$. (*C*) i-tRAP analysis of the charging ratios of $tRNA^{Gln}$(CUG) (*left*) and $tRNA^{Gly}$(GCC) (*right*) under amino acid starvation. tRNA was extracted from young TIG-1 cells that had been cultured in an amino acid–free medium, which was replaced with a medium containing amino acids followed by a 1 h of incubation. Data, mean ± SEM; $n = 6$; statistics, unpaired two-tailed Student's *t*-test. (*) $P < 0.05$; NS, not significant. (*D*) Analysis of $tRNA^{Gln}$(CUG) and $tRNA^{Gly}$(GCC) aminoacylation by northern blotting. Small RNA was extracted from TIG-1 cells that had been cultured in an amino acid–free medium, which was replaced with a medium containing amino acids followed by incubation for 1 h. Aminoacylation of $tRNA^{Gln}$(CUG) and $tRNA^{Gly}$(GCC) were analyzed by acid-urea gel electrophoresis and subsequent northern blot hybridization using probes for $tRNA^{Gln}$(CUG) and $tRNA^{Gly}$(GCC), respectively. tRNA charging levels were quantified as a ratio of charged-to-total tRNA. Data, means ± SEM; $n = 3$. (*E*) Charging ratios of $tRNA^{Gln}$(CUG) in young and old TIG-1 cells cultured in an amino acid–free medium for 15 h. Data, means ± SEM; $n = 8$; statistics, unpaired two-tailed Student's *t*-test. (*) $P < 0.05$.

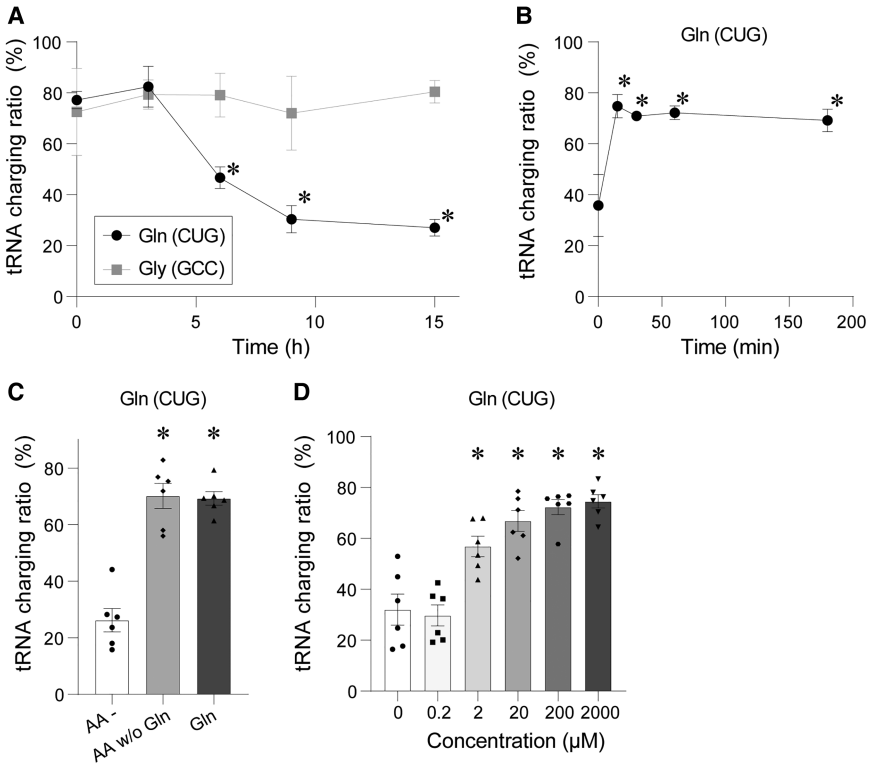

FIGURE 5. Charging dynamics of tRNA^{Gln}(CUG). (*A*) Charging ratios of tRNA^{Gln}(CUG) and tRNA^{Gly}(GCC) in TIG-1 cells after amino acid starvation. (*B*) Recharging ratios of tRNA^{Gln}(CUG) in TIG-1 cells after amino acid supplementation. (*C*) Charging ratios of tRNA^{Gln}(CUG) in TIG-1 cells after supplementation with amino acids except glutamine, or with only 2 mM glutamine. AA w/o Gln medium was prepared using MEM essential amino acids solution and MEM nonessential amino acids solution (Wako). AA −, amino acid-starved condition. (*D*) Charging ratios of tRNA^{Gln}(CUG) in TIG-1 cells after supplementation of glutamine at indicated concentrations in an amino acid–free medium for 1 h. Data, mean ± SEM; $n = 5$ (*A*,*B*) and 6 (*C*,*D*); statistics, (*A*,*B*) one-way ANOVA ([*] $P < 0.05$ versus 0 h), (*C*,*D*) one-way ANOVA ([*] $P < 0.05$).

been developed to measure the charging ratio of tRNA. For example, northern blotting has been popularly used to examine the charging ratio of individual tRNAs. Although careful selection of hybridization temperature and use of locked nucleic acid–modified probes allows highly sensitive and specific detection of RNA by northern blotting (Várallyay et al. 2008), few laboratories today possess such technics and equipment. When the charging ratio was calculated by northern blot, the value came out higher than that of i-tRAP. The differences may be derived from the methodological principles of northern blot and i-tRAP. i-tRAP can be performed in many labs as far as real-time qPCR systems are available, while northern blot requires special techniques or equipment. A PCR-based method for measuring the charging ratio of tRNA has already been developed (Loayza-Puch et al. 2016), which can analyze changes in the charging ratio of tRNA in a given sample relative to another reference sample. In contrast, the i-tRAP method can directly measure tRNA charging ratios and does not require reference samples, making it possible to compare the charging ratios of tRNA between different experiments and different types of tRNAs. Additionally, the qPCR-based i-tRAP method, which can easily be performed with dozens of samples, could measure the tRNA charging ratio precisely at the individual tRNA level (Fig. 1B). As far as tRNA^{Gln} is concerned, it was possible to identify differences in the target sequence of the MGB probe (i.e., Gln (CTG)-6 and Gln (TTG)-1), but was difficult to identify differences in the target sequence of the forward primer (i.e., Gln (CTG)-2). In general, internal mismatches between primers and targeted DNA can be tolerated (Kwok et al. 1990), whereas this low specificity could be improved by careful selection of annealing temperature and primer sequences. The efficiency of identifying tRNAs with highly similar sequences depends on the primer/probe set and should be pretested using synthesized DNA corresponding to the specific tRNA sequence. Careful consideration should be given to experimental conditions, since the choice of enzyme and the demethylation process could change the stability of the results and sensitivity of the methods. By careful selections of these conditions, i-tRAP can measure the charging ratio of tRNA easily.

Although the charging ratios of most tRNAs were maintained under prolonged amino acid starvation in both young and old cells, the charging ratio of tRNA^{Gln} drastically changed in response to nutrient status. The charging dynamics of tRNA seem to vary depending on species and cellular types. Studies using proliferative species, such as *E. coli* (Sørensen 2001; Dittmar et al. 2005) and yeast (Zaborske et al. 2009), reported fast and global reduction in the charging ratios of tRNA after starvation. Our study showed a specific change in tRNA^{Gln} charging in human TIG-1 cells, as previously observed in MEF and human kidney and pancreatic cancer cell lines (Pavlova et al. 2020). However, the effect of amino acid starvation on tRNA charging in HEK293 is quite different (Saikia et al. 2016).

The concentrations of tRNA-charged amino acids are the result of consumption for protein synthesis and supply as reviewed in (Rubio Gomez and Ibba 2020). Glutamine is a well-known stimulant of protein synthesis and cellular proliferation, since glutamine is greatly consumed as a precursor for other amino acids (MacLennan et al. 1987). In

MEF, the concentrations of glutamine also significantly decrease under amino acid starvation conditions (Pavlova et al. 2020). As a nonessential amino acid, the cellular levels of glutamine fluctuate dynamically between consumption and biogenesis in response to nutrients and the external environment.

i-tRAP method is sensitive enough to detect senescence-associated dynamics of the charging ratio of $tRNA^{Gln}$(CUG). We showed that the charging ratio of a $tRNA^{Gln}$(CUG) was lower in senescent cells only in amino acid starvation conditions. The reasons and effects of a low charging ratio of $tRNA^{Gln}$(CUG) in senescent cells are speculative. Accumulation of abnormal aaRS during senescence is reported (Hosbach and Kubli 1979; Takahashi et al. 1985) and may decrease the charging ratio of tRNA. A low charging ratio of $tRNA^{Gln}$(CUG), in turn, may also suppress protein synthesis in senescent cells. These questions compose key directions toward the elucidation of senescence mechanisms.

In conclusion, we developed i-tRAP, an efficient and convenient method for analyzing tRNA charging. We showed that this method has high specificity for isoacceptor tRNAs and broad applicability for the qualification of different tRNA charging. Besides in cultured cells, i-tRAP will advance biology through the quantification of tRNA charging in tissue levels. As the demand for measuring tRNA charging is constantly being expanded, i-tRAP will provide a much-needed simple method for analyzing tRNA charging.

MATERIALS AND METHODS

Human mature tRNA sequences

Sequences of tRNAs were referred from the Genomic tRNA Database (http://lowelab.ucsc.edu/GtRNAdb/) (Chan and Lowe 2016) and the mitochondrial genome sequence (NC_012920) (Andrews et al. 1999).

Cell culture and RNA isolation

Human embryonic kidney 293 (HEK293) (JCRB9068, JCRB Cell Bank) and TIG-1 (spontaneously developed diploid fibroblast cell lines of fetal lung [JCRB0501, JCRB Cell Bank]) cells were cultured in Dulbecco's Modified Eagle's Medium (DMEM, Nacalai Tesque) with 10% supplemented with fetal bovine serum (Gibco). Human primary lung (PCS-201-013, ATCC), adult dermal (PCS-201-012, ATCC) and neonatal dermal cells (PCS-201-010, ATCC) were cultured in the recommended media. Cells were maintained at 37°C in a humidified chamber supplemented with 5% CO_2. For tRNAseq and northern blot, 3.0–6.0 × 10^6 cells were seeded on 100 mm dishes using a culture medium. For i-tRAP and RT-qPCR, 4.0–8.0 × 10^5 cells were seeded on six well plates.

For amino acid starvation, cells were cultured in amino acid–free DMEM (Wako) supplemented with 0.5% dialyzed fetal bovine serum (Gibco) for indicated time. Amino acid supplementation was conducted using MEM essential amino acids solution, MEM nonessential amino acids solution, and 200 mM glutamine solution (Wako) for the indicated time.

Small RNA was extracted from cells using Isogen II reagent (Nippongene) and Ethachinmate (Nippongene) according to manufacturer's instruction.

Periodate oxidation, β-elimination and end repair

Periodate oxidation of RNA was carried out as described previously with modification (Evans et al. 2017). Briefly, small RNA was oxidized in 100 mM CH_3COONa, pH 5.2 and freshly prepared 50 mM $NaIO_4$ at 27°C for 30 min. The reaction was quenched using 100 mM glucose at 27°C for 5 min. To purify tRNA and remove periodate, resultant RNA was separated by electrophoresis using a 15% denaturing polyacrylamide gel (5 M Urea, 1× TBE, Bio-craft). tRNA, which contained periodated 3′CC tRNA and charged 3′CCA tRNA, was excised and eluted from the gel in TE buffer, and precipitated with ethanol. For β-elimination for removing the oxidized 3′A residue and leaving a phosphate at the terminal 3′C residue, and deacylation, purified tRNA was treated with 200 mM Tris-HCl, pH 9.0, at 75°C for 5 min followed by ethanol precipitation. Then, tRNA was treated with T4 polynucleotide kinase (Thermo Fisher Scientific) at 37°C for 30 min to remove 3′-phosphate (end repair), followed by ethanol precipitation.

Demethylation reactions

Demethylation reaction was carried out as previously described with modifications (Zheng et al. 2015). Briefly, truncated wild-type and D135S mutant AlkB with deletion of the amino-terminal 11 amino acids was cloned into a pETBA vector (Biodynamics Laboratory) and overexpressed in Zip Competent Cell BL21 (DE3) (Biodynamics Laboratory). Cells were grown at 37°C in the presence of 50 μM ampicillin until the OD600 reached 0.5–0.6. After the addition of 1 mM IPTG and 5 μM $FeSO_4$, cells were incubated for an additional 4 h at 30°C. Cells were collected, pelleted and resuspended in PBS with protease inhibitor (cOmplete, Mini, EDTA-free, Roche). Then, cells were lysed by sonication and centrifuged at 3000*g* for 10 min. The soluble proteins were purified using HisTrap FF crude (Cytiva) at 4°C. The reaction buffer contained 300 mM KCl, 2 mM $MgCl_2$, 50 μM $(NH4)_2Fe(SO_4)_2{\cdot}6H_2O$, 300 μM 2-ketoglutarate, 2 mM l-ascorbic acid, 50 μg/mL BSA, 50 mM MES buffer (pH 5.0). A total of 40 pmol of tRNA was treated with 80 pmol WT AlkB and 160 pmol D135S AlkB in the reaction buffer, and the reaction mixture was incubated at 27°C for 2 h.

tRNA sequencing for measuring charging ratios

tRNA sequencing was performed as previously described with modifications (Evans et al. 2017). Briefly, 100 ng of tRNA treated with periodate oxidation, β-elimination, deaminoacylation, end repair and demethylation, as described above, was used as a template for a library. The template-switching and reverse transcription reactions were done as described (Xu et al. 2019) using TGIRT (InGex) with 5′ labeled TGIRT primers (T- and G-ending, Supplemental Table S1) annealed to complementary RNA (5′-AAGAUCGGAAGAGCACACGUCUGAACUCCAGUCAC-3′). The

products were purified by using a MinElute Reaction Cleanup Kit (Qiagen). The R1R DNA adapter (Supplemental Table S1) was preadenylated by using an adenylation kit (New England Biolabs) and then ligated to the 3′ end of the cDNA by using thermostable 5′ App DNA/RNA Ligase (New England Biolabs) for 16 h at 65°C. The ligated products were purified by using a MinElute Reaction Cleanup Kit and amplified by PCR with Phusion High-Fidelity DNA polymerase (Thermo Fisher Scientific; denaturation at 98°C for 5 sec followed by 15 cycles of 98°C 5 sec, 60°C 10 sec, 72°C 15 sec and then held at 4°C). The PCR products were cleaned up by using Agencourt AMPure XP beads (Beckman Coulter) and size selection of the library was performed using Pippin Prep automated gel system (175–300 bp, Sage science). Concentration of cDNA libraries was quantified using a GenNext NGS Library Quantification Kit (TOYOBO). Sequencing was performed on an Illumina Nextseq 500 platform in a 150-base single-end mode (illumina). The output data was demultiplexed and BCL-to-Fastq conversion was performed using Illumina's bcl2fastq software.

The sequenced read was mapped to the human tRNA sequences using Blast version 2.2.26, and was aligned to the 25 nt of 3′ end of tRNA sequences without any mismatches. The aligned read with 3′-end CCA was regarded to be derived from charged tRNA, whereas the read ended with 3′-end CC was from uncharged tRNA. Charging ratios were determined as 3′-end CCA-aligned reads over the sum of 3′-end CCA- and CC-aligned reads. The tRNAseq data sets are available at the Gene Expression Omnibus (GEO) with accession number GSE188862. Use tokens kvercucarnelhuv.

Ligation of an adaptor to tRNA for i-tRAP

Adenylated Linker, a 5′ adenylated adaptor with 3′-end block, was purchased from PerkinElmer (5′-rAppCAGTAGGC ACCATCAAT/3ddC/-3′). Chemically and enzymatically pretreated tRNA (300 ng) were mixed with adenylated adapter (20 pmol), and then incubated with ligation mixture containing 2 µL of 10× reaction buffer and 1 unit of truncated T4 Rnl2 (New England Biolabs) in 20 µL of total volume at 37°C for 60 min.

Preparation of DNA fragments containing tRNA sequences for generation of standard curves

In preparation of PCR products that contain tRNA sequences, four kinds of oligonucleotides per tRNA were designed as shown in Supplemental Table S2 (Fasmac). First forward (1F) oligonucleotide was 37 nt containing a linker sequence, and second, third, and fourth reverse primers (2R, 3R, and 4R) were 33–37 nt containing the tRNA sequence. For producing a DNA fragment of 3′CCA-tRNA, the 2R oligonucleotide was used, and for producing a DNA fragment of 3′CC-tRNA, the 3R oligonucleotide was used. The mixture for the extension reaction contained the three kinds of oligonucleotides (3′CCA-tRNA: 1F, 2R, 3R; 3′CC-tRNA: 1F, 3R, 4R; 25 pmol each) and 12.5 µL of KOD One PCR Master Mix-Blue- (TOYOBO) in 25 µL. The mixture was incubated at 98°C for 60 sec, followed by 12 cycles of 10 sec at 98°C, 5 sec at 60°C, and 5 sec at 68°C. Using 10 µL of the resulting reaction mixture as a template, PCR was performed containing 1F and 3R, or 1F and 4R oligonucleotides (100 pmol) in 200 µL of the reaction mixture. The mixture was incubated at 98°C for 60 sec, followed by 40 cycles of 10 sec at 98°C, 5 sec at 60°C, and 5 sec at 68°C. The PCR products were electrophoresed on a 2% agarose gel and visualized by staining with Midori Green Direct (Nippon Genetics). The desired DNA obtained from the agarose gel was purified with a QIAquick Gel Extraction Kit (Qiagen) and eluted with 30 µL of the elution buffer. The purified PCR product concentration was determined using NanoDrop 2000 (Thermo Fisher Scientific). Two kinds of PCR products were then combined at several ratios (3′CCA-tRNA: 3′CC-tRNA; 10:90, 20:80, 30:70, 40:60, 50:50, 60:40, 70:30, 80:20, and 90:10) and used for the establishment of the standard curve in qPCR as described below. The total concentration of standard solution was adjusted to 1 ag/µL for establishing the linear calibration curve.

qRT-PCR system and procedure for detecting individual tRNA-acylation using PCR (i-tRAP)

Adapter-ligated RNAs were incubated at 95°C for 5 min to denature, and then placed on ice. The denatured adaptor-ligated RNAs were reverse-transcribed using ReverTra Ace (TOYOBO) using a reverse transcription (RT) primer (Supplemental Table S1). The sequence of RT primer was based on the sequences of the adenylated linker and an additional sequence from nonhuman species (*Gryllus bimaculatus*) (Tsukamoto and Nagata 2016), since tRNA sequence as a template is too short to prepare a primer and probe set for qPCR. RT reaction was performed at 42°C for 60 min. The resultant cDNA solution was diluted with water by 1:5, and 1 µL of this solution was added to the real-time PCR mixture containing 5 µL of 2× TaqMan Genotyping Master Mix (Thermo Fisher Scientific), 0.4 µL of Custom TaqMan SNP Genotyping Assays containing specific primers and probes (Supplemental Table S3) (Thermo Fisher Scientific), and 3.6 µL of distilled water. 7900HT Real-Time PCR System (Thermo Fisher Scientific) was used to determine the threshold cycles (C_t). The cycling conditions were as follow: initial denaturation for 10 min at 95°C, 40 or 50 cycles of 5 sec at 95°C, and 60 sec at 60°C. Fluorescence signals were collected at the 60°C step of each cycle. All reactions were run in duplicate and the threshold cycles were determined.

Quantitative RT-PCR

Large RNA from the cells which were extracted using Isogen II (Nippon gene) or TRIzol (Thermo Fisher Scientific) according to the manufacturer's protocol was used as the template. Extracted RNA was treated with RQ1 DNase I (Promega) at 37°C for 30 min. The RNA quality and quantity were determined by a NanoDrop 2000 (Thermo Fisher Scientific). Then, RNA (300 ng each) was reverse-transcribed using a SuperScript VILO cDNA Synthesis Kit (Thermo Fisher Scientific). The reverse transcription mixture was incubated at 42°C for 60 min. The resultant cDNA solution was diluted with water by 1:5, and 1 µL of this solution was added to the real-time PCR mixture containing 5 µL of 2× GeneAce SYBR qPCR Mix α (Nippon gene), 0.5 µL of each primer in 10 µM, and 3 µL of H_2O. 7900HT Real-Time PCR System (Thermo Fisher Scientific) was used. The cycling conditions were as follows: initial denaturation for 10 min at 95°C, 40 cycles of 15 sec at 95°C, 30 sec at 60°C. Fluorescence signals were collected at the 60°C step of each cycle. All reactions

were run in duplicate and the C_t values were determined. The expression levels of target genes were normalized to the expression levels of *ActB*. To evaluate the reaction using the ΔC_t method, we used a primer set shown in Supplemental Table S4.

Acid urea PAGE followed by northern blot analysis

An amount of 3000 ng of small RNA was mixed with an equal volume of acid urea dye (0.1 M sodium acetate [pH 5.2], 8 M urea, 0.05% bromophenol blue, 0.05% xylene cyanol) and resolved on a 5 M acid urea PAGE gel (12%) in 100 mM sodium acetate (pH 5.2) and 2 mM EDTA. Preelectrophoresis was performed at 4°C for 30 min at 20 mA. The sample was separated under 250 V for 960 min at 4°C. The gel was electroblotted onto a positively charged nylon membrane (Hybond N+, Cytiva) using an electroblot apparatus at 10 V for 120 min with 40 mM Tris-HCl (pH 8.0) and 2 mM EDTA (pH 8.0) as transfer buffer. The membrane was rinsed briefly with 2× saline sodium citrate buffer (SSC) and UV cross-linked at 120 mJ/cm^2. The membrane was incubated in DIG Easy Hyb (Roche) at 52°C for 1 h and then hybridized with 10 nM probe in DIG Easy Hyb solution at 52°C overnight. A probe was labeled with the nonradioactive DIG, using an End Tailing Kit (Roche). The probe sequence was for the human tRNA^{Gln}(CUG) (5′-GAGATTTGAACTCGGATCGCTGGAT-3′) and tRNA^{Gly}(GCC) (5′-TGCATGGGCCGGGAATCGAACCCGGGCCTCCCGCG-3′). The membrane was washed at room temperature twice using a low stringency buffer solution (2× SSC, 0.1% SDS), and at 52°C twice using a high stringency buffer solution (0.5× SSC, 0.1% SDS) for 5 and 10 min. The subsequent steps were done at room temperature. Membranes were washed in the washing buffer containing 0.1 M maleic acid-NaOH, pH 7.5, 0.15 M NaCl and 0.3% (v/v) Tween 20 for 5 min and blocked in 1× DIG Northern starter kit blocking solution (Roche) for 30 min. This was followed by incubation with anti-digoxigenin-AP (1:10,000 in blocking solution) for 30 min and twice washes with the washing buffer, 15 min each. Membranes were finally rinsed in the detection buffer (0.1 M Tris-HCl, pH 9.5, and 0.1 M NaCl) for 5 min and chemiluminescence was detected using CDP-Star reagent and an ImageQuant LAS 500 (Cytiva).

ImageJ software was used for quantification. Briefly, the area around each band was specified by rectangular selection in the program tools and quantifies the intensity of each band. tRNA charging levels were quantified as a ratio of charged-to-total tRNA.

Western blotting

TIG-1 cells lysed with RIPA buffer (Thermo Fisher Scientific) supplemented with protease inhibitor cocktail (Merck). After centrifugation at 20,400*g* for 10 min, supernatant was collected. Protein was quantified using a BCA protein assay kit (Thermo Fisher Scientific). Sample buffer was directly added to the sample and boiled for 10 min. Samples were separated on SuperSep Ace 5%–12% gel (Wako), transferred onto a PVDF membrane (Immobilon-P; Merck), and probed using rabbit anti-QARS (Bethyl Laboratories, A304-752A) or anti-β-actin antibody (Sigma, #A5316). Later, the membranes were rinsed 3 times in 1 x TBST and incubated with HRP-conjugated secondary antibody. Signals were detected using Chemi-Lumi One Super (Nacalai Tesque) and an ImageQuant LAS 500 (Cytiva).

Bands were quantified with ImageJ. Briefly, the area around each band was specified by rectangular selection in the program tools and quantifies the intensity of each band. QARS protein levels were normalized to β-actin.

Improved tRNA RT method using TGIRT

The tRNA RT reaction was performed as previously described with modifications (Behrens et al. 2021). Briefly, the denatured adaptor-ligated RNAs without demethylase treatment were reverse-transcribed using TGIRT (InGex). TGIRT reactions were performed in a 20 µL final volume by combining the template and RT primer (Supplemental Table S1) with 10U SUPERase In (Thermo Fisher Scientific), 5 mM DTT and low salt buffer (50 mM Tris-HCl (pH 8.3), 75 mM KCl, 3 mM $MgCl_2$). After TGIRT addition, samples were incubated at 42°C for 10 min. After addition of dNTPs to a final concentration of 1 mM, samples were incubated at 42°C for 16 h.

Improved tRNA RT method using SuperScript IV

tRNA RT reaction was performed as previously described with modifications (Watkins et al. 2022). Briefly, the denatured adaptor-ligated RNAs without demethylase treatment was reverse-transcribed using SuperScript IV Reverse Transcriptase (Thermo Fisher Scientific). RT reactions were performed in a 20 µL final volume by combining the template and RT primer (Supplemental Table S1) with 40U RNaseOUT (Thermo Fisher Scientific), 5 mM DTT, 1 mM dNTPs and 5× SuperScript IV buffer. After the initial 10 min incubation at 55°C for 10 min, samples were incubated at 35°C for 16 h.

Statistics

Either two-tailed *t*-test or one-way ANOVA with Bonferroni's post-hoc test was used. Statistical analysis was performed using GraphPad Prism 8 (GraphPad Software). Statistical significance was defined as $P < 0.05$.

SUPPLEMENTAL MATERIAL

Supplemental material is available for this article.

COMPETING INTEREST STATEMENT

T.K. and Y.T. are preparing a patent application related to the work in this manuscript.

ACKNOWLEDGMENTS

We thank Dr. Takefumi Kondo, Kyoto University, for technical advice, and Terashi Yukie and Keiko Yamasaki, NIBIOHN, for technical support. This work was in part supported by grants from the Japan Agency of Medical Research and Development (AMED, JP21gm5010001).

Received June 21, 2022; accepted October 13, 2022.

REFERENCES

Andrews RM, Kubacka I, Chinnery PF, Lightowlers RN, Turnbull DM, Howell N. 1999. Reanalysis and revision of the Cambridge reference sequence for human mitochondrial DNA. *Nat Genet* **23:** 147. doi:10.1038/13779

Avcilar-Kucukgoze I, Bartholomäus A, Cordero Varela JA, Kaml RF-X, Neubauer P, Budisa N, Ignatova Z. 2016. Discharging tRNAs: a tug of war between translation and detoxification in *Escherichia coli*. *Nucleic Acids Res* **44:** 8324–8334. doi:10.1093/nar/gkw697

Behrens A, Rodschinka G, Nedialkova DD. 2021. High-resolution quantitative profiling of tRNA abundance and modification status in eukaryotes by mim-tRNAseq. *Mol Cell* **81:** 1802–1815.e7. doi:10.1016/j.molcel.2021.01.028

Chan PP, Lowe TM. 2016. GtRNAdb 2.0: an expanded database of transfer RNA genes identified in complete and draft genomes. *Nucleic Acids Res* **44:** D184–D189. doi:10.1093/nar/gkv1309

Crick FH. 1958. On protein synthesis. *Symp Soc Exp Biol* **12:** 138–163.

Crick F. 1970. Central dogma of molecular biology. *Nature* **227:** 561–563. doi:10.1038/227561a0

Dittmar KA, Sørensen MA, Elf J, Ehrenberg M, Pan T. 2005. Selective charging of tRNA isoacceptors induced by amino-acid starvation. *EMBO Rep* **6:** 151–157. doi:10.1038/sj.embor.7400341

Elf J, Nilsson D, Tenson T, Ehrenberg M. 2003. Selective charging of tRNA isoacceptors explains patterns of codon usage. *Science* **300:** 1718–1722. doi:10.1126/science.1083811

Evans ME, Clark WC, Zheng G, Pan T. 2017. Determination of tRNA aminoacylation levels by high-throughput sequencing. *Nucleic Acids Res* **45:** e133. doi:10.1093/nar/gkx514

Gabius H-J, Goldbach S, Graupner G, Rehm S, Cramer F. 1982. Organ pattern of age-related changes in the aminoacyl-tRNA synthetase activities of the mouse. *Mech Ageing Dev* **20:** 305–313. doi:10.1016/0047-6374(82)90098-7

Gobet C, Weger BD, Marquis J, Martin E, Neelagandan N, Gachon F, Naef F. 2020. Robust landscapes of ribosome dwell times and aminoacyl-tRNAs in response to nutrient stress in liver. *Proc Natl Acad Sci* **117:** 9630–9641. doi:10.1073/pnas.1918145117

Gong S, Peng Y, Jiang P, Wang M, Fan M, Wang X, Zhou H, Li H, Yan Q, Huang T, et al. 2014. A deafness-associated $tRNA^{His}$ mutation alters the mitochondrial function, ROS production and membrane potential. *Nucleic Acids Res* **42:** 8039–8048. doi:10.1093/nar/gku466

Gong S, Wang X, Meng F, Cui L, Yi Q, Zhao Q, Cang X, Cai Z, Mo JQ, Liang Y, et al. 2020. Overexpression of mitochondrial histidyl-tRNA synthetase restores mitochondrial dysfunction caused by a deafness-associated $tRNA^{His}$ mutation. *J Biol Chem* **295:** 940–954. doi:10.1016/S0021-9258(17)49906-6

Goodenbour JM, Pan T. 2006. Diversity of tRNA genes in eukaryotes. *Nucleic Acids Res* **34:** 6137–6146. doi:10.1093/nar/gkl725

Ho YS, Kan YW. 1987. In vivo aminoacylation of human and *Xenopus* suppressor tRNAs constructed by site-specific mutagenesis. *Proc Natl Acad Sci* **84:** 2185–2188. doi:10.1073/pnas.84.8.2185

Hoagland MB, Stephenson ML, Scott JF, Hecht LI, Zamecnik PC. 1958. A soluble ribonucleic acid intermediate in protein synthesis. *J Biol Chem* **231:** 241–257. doi:10.1016/S0021-9258(19)77302-5

Hosbach HA, Kubli E. 1979. Transfer RNA in aging *Drosophila*: I. extent of aminoacylation. *Mech Ageing Dev* **10:** 131–140. doi:10.1016/0047-6374(79)90076-9

Kwok S, Kellogg DE, Mckinney N, Spasic D, Goda L, Levenson C, Sninsky JJ. 1990. Effects of primer-template mismatches on the polymerase chain reaction: human immunodeficiency virus type 1 model studies. *Nucleic Acids Res* **18:** 999–1005. doi:10.1093/nar/18.4.999

Kwon NH, Fox PL, Kim S. 2019. Aminoacyl-tRNA synthetases as therapeutic targets. *Nat Rev Drug Discov* **18:** 629–650. doi:10.1038/s41573-019-0026-3

Loayza-Puch F, Rooijers K, Buil LCM, Zijlstra J, Oude Vrielink JF, Lopes R, Ugalde AP, Van Breugel P, Hofland I, Wesseling J, et al. 2016. Tumour-specific proline vulnerability uncovered by differential ribosome codon reading. *Nature* **530:** 490–494. doi:10.1038/nature16982

MacLennan PA, Brown RA, Rennie MJ. 1987. A positive relationship between protein synthetic rate and intracellular glutamine concentration in perfused rat skeletal muscle. *FEBS Lett* **215:** 187–191. doi:10.1016/0014-5793(87)80139-4

Morris DW, DeMoss JA. 1965. Role of aminoacyl-transfer ribonucleic acid in the regulation of ribonucleic acid synthesis in *Escherichia coli*. *J Bacteriol* **90:** 1624–1631. doi:10.1128/jb.90.6.1624-1631.1965

Nagy A, Vitásková E, Černíková L, Křivda V, Jiřincová H, Sedlák K, Horníčková J, Havlíčková M. 2017. Evaluation of TaqMan qPCR system integrating two identically labelled hydrolysis probes in single assay. *Sci Rep* **7:** 41392. doi:10.1038/srep41392

Neu HC, Heppel LA. 1964. Nucleotide sequence analysis of polyribonucleotides by means of periodate oxidation followed by cleavage with an amine. *J Biol Chem* **239:** 2927–2934. doi:10.1016/S0021-9258(18)93834-2

Ohashi M, Aizawa S, Ooka H, Ohsawa T, Kaji K, Kondo H, Kobayashi T, Noumura T, Matsuo M, Mitsui Y, et al. 1980. A new human diploid cell strain, TIG-1, for the research on cellular aging. *Exp Gerontol* **15:** 121–133. doi:10.1016/0531-5565(80)90083-2

Pavlova NN, King B, Josselsohn RH, Violante S, Macera VL, Vardhana SA, Cross JR, Thompson CB. 2020. Translation in amino-acid-poor environments is limited by $tRNA^{Gln}$ charging. *Elife* **9:** e62307. doi:10.7554/eLife.62307

Rubio Gomez MA, Ibba M. 2020. Aminoacyl-tRNA synthetases. *RNA* **26:** 910–936. doi:10.1261/rna.071720.119

Saikia M, Wang X, Mao Y, Wan J, Pan T, Qian S-B. 2016. Codon optimality controls differential mRNA translation during amino acid starvation. *RNA* **22:** 1719–1727. doi:10.1261/rna.058180.116

Sam S-S, Teoh B-T, Chee C-M, Mohamed-Romai-Noor N-A, Abd-Jamil J, Loong S-K, Khor C-S, Tan K-K, AbuBakar S. 2018. A quantitative reverse transcription-polymerase chain reaction for detection of Getah virus. *Sci Rep* **8:** 17632. http://dx.doi.org/10.1038/s41598-018-36043-6.

Sørensen MA. 2001. Charging levels of four tRNA species in *Escherichia coli* Rel^+ and Rel^- strains during amino acid starvation: a simple model for the effect of ppGpp on translational accuracy. *J Mol Biol* **307:** 785–798. doi:10.1006/jmbi.2001.4525

Takahashi R, Mori N, Goto S. 1985. Alteration of aminoacyl tRNA synthetases with age: accumulation of heat-labile enzyme molecules in rat liver, kidney and brain. *Mech Ageing Dev* **33:** 67–75. doi:10.1016/0047-6374(85)90109-5

Trewick SC, Henshaw TF, Hausinger RP, Lindahl T, Sedgwick B. 2002. Oxidative demethylation by *Escherichia coli* AlkB directly reverts DNA base damage. *Nature* **419:** 174–178. doi:10.1038/nature00908

Tsukamoto Y, Nagata S. 2016. Newly identified allatostatin Bs and their receptor in the two-spotted cricket, *Gryllus bimaculatus*. *Peptides* **80:** 25–31. doi:10.1016/j.peptides.2016.03.015

Várallyay E, Burgyán J, Havelda Z. 2008. MicroRNA detection by northern blotting using locked nucleic acid probes. *Nat Protoc* **3:** 190–196. doi:10.1038/nprot.2007.528

Watkins CP, Zhang W, Wylder AC, Katanski CD, Pan T. 2022. A multiplex platform for small RNA sequencing elucidates multifaceted tRNA stress response and translational regulation. *Nat Commun* **13:** 2491. doi:10.1038/s41467-022-30261-3

Webster GC, Webster SL. 1981. Aminoacylation of tRNA by cell-free preparations from aging *Drosophila melanogaster*. *Exp Gerontol* **16:** 487–494. doi:10.1016/0531-5565(81)90030-9

Xu H, Yao J, Wu DC, Lambowitz AM. 2019. Improved TGIRT-seq methods for comprehensive transcriptome profiling with

decreased adapter dimer formation and bias correction. *Sci Rep* **9:** 7953. doi:10.1038/s41598-019-44457-z

Zaborske JM, Narasimhan J, Jiang L, Wek SA, Dittmar KA, Freimoser F, Pan T, Wek RC. 2009. Genome-wide analysis of tRNA charging and activation of the eIF2 kinase Gcn2p. *J Biol Chem* **284:** 25254–25267. doi:10.1074/jbc.M109.000877

Zheng G, Qin Y, Clark WC, Dai Q, Yi C, He C, Lambowitz AM, Pan T. 2015. Efficient and quantitative high-throughput tRNA sequencing. *Nat Methods* **12:** 835–837. doi:10.1038/nmeth.3478

Zhou Y, Goodenbour JM, Godley LA, Wickrema A, Pan T. 2009. High levels of tRNA abundance and alteration of tRNA charging by bortezomib in multiple myeloma. *Biochem Biophys Res Commun* **385:** 160–164. doi:10.1016/j.bbrc.2009.05.031

MEET THE FIRST AUTHOR

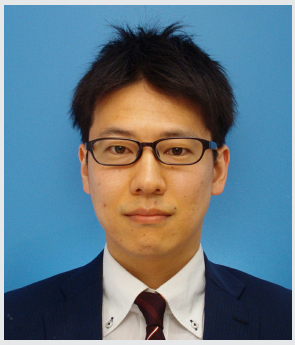

Yusuke Tsukamoto

***Meet the First Author(s)* is a new editorial feature within *RNA*, in which the first author(s) of research-based papers in each issue have the opportunity to introduce themselves and their work to readers of *RNA* and the RNA research community. Yusuke Tsukamoto is the first author of this paper, "i-tRAP (individual tRNA acylation PCR): a convenient method for selective quantification of tRNA charging." Yasuke is a postdoctoral fellow in the laboratory of Dr. Kimura at the National Institutes of Biomedical Innovation, Health and Nutrition, in the KAGAMI project. Yasuke's work focuses on the physiology and metabolism of D-amino acids.**

What are the major results described in your paper and how do they impact this branch of the field?

This paper developed a method called i-tRAP to quantify individual tRNA charging ratios. In this method, we utilized demethylases to remove base methylations which are problematic for a reverse transcription reaction, and a β-elimination reaction to remove the 3′ adenosine residue in uncharged tRNA and TaqMan MGB qRT-PCR. Our developed i-tRAP can distinguish between the cDNA of charged tRNA and uncharged tRNA.

What led you to study RNA or this aspect of RNA science?

Since joining Dr. Kimura's lab for my postdoc, I have focused on D-amino acid metabolism and biological function. The question of whether D-amino acids are used in translation led us to perform tRNAseq, and we unexpectedly found that $tRNA^{Gln}$ displayed the largest change in response to amino acid starvation. For further investigation, it was necessary to measure the charging ratio of individual tRNAs, and we developed the method reported here.

During the course of these experiments, were there any surprising results or particular difficulties that altered your thinking and subsequent focus?

It was difficult to obtain high-quality cDNA of tRNA, so we considered several methods besides the methods shown in this paper. Unfortunately, we could not obtain high-quality cDNA by using most of them. We believed in the importance of developing the method of measuring tRNA charging levels and we were committed to find out the experimental results. Ultimately, we created a technique that could be applied to a variety of studies.

What are some of the landmark moments that provoked your interest in science or your development as a scientist?

When I was a high school student, my teacher gave me the book, *Between organic and inorganic matter*, by Dr. Shin-Ichi Fukuoka, and it really stirred my imagination and made me want to know more. The book induced my interest toward biology and I decided not only to read scientific articles but also to do my own research.

Are there specific individuals or groups who have influenced your philosophy or approach to science?

One of the many people that influenced my philosophy and approach to science was my PhD advisor, Professor Shinji Nagata. He showed me how to plan for the experiments and how to do the experiments. He taught me the fundamentals of scientific approaches and it encouraged me to continue doing research. I cannot thank him enough for the impact he had on me as a novice researcher.